ELSEVIER

Cement & Concrete Composites 23 (2001) 485–493

Cement & Concrete Composites

www.elsevier.com/locate/cemconcomp

The influence of metakaolin and silica fume on the chemistry of alkali–silica reaction products

W. Aquino [a,*], D.A. Lange [a], J. Olek [b]

[a] University of Illinois, Urbana-Champaign, Urbana, IL 61801, USA
[b] Purdue University, USA

Abstract

This investigation studies the influence of two mineral admixtures, silica fume (SF) and high-reactivity metakaolin (HRM), on the chemistry of alkali–silica reaction (ASR) products. Four different mortar bar mixes containing different combinations of high-alkali cement, alkali–inert dolomitic limestone, reactive Beltane opal, HRM, and SF were prepared and stored in a 1 N NaOH solution at 80°C (ASTM C 1260) for 21 days. Expansion of bar specimens was measured, and chemical analysis was performed at different ages using X-ray spectra and maps. Test results confirmed that HRM and SF significantly reduce expansion due to ASR. In addition, X-ray microanalysis showed that calcium content increases with time in ASR products. Furthermore, it was found that as ASR proceeded the calcium content of reaction products increased proportionally as the silica content decreased.

Keywords: Alkali–silica reaction; Calcium; Pozzolans; Metakaolin; Silica fume

1. Introduction

Alkali–silica reaction (ASR) has become one of the most challenging problems in concrete technology today. Due to environmental concerns, changes in the manufacturing process of portland cement have led to increases in its alkali content. In addition, sources of non-alkali reactive aggregates are being depleted around the world. This combination of factors has set favorable scenarios for ASR to occur more frequently.

It is important that engineers and materials scientists understand the basic mechanisms behind ASR, so that viable solutions to control and eradicate this reaction can be devised. So far, there is no general agreement as to the exact nature of the mechanisms behind ASR, and the solutions that have been implemented to date are often justified by limited empirical data. Although extensive research has probed the subject, some important questions remain unanswered. For instance, the role of calcium, potassium, and sodium ions in the ASR expansion process is still a matter of debate [1–4].

Mineral pozzolanic admixtures such as fly ash, silica fume (SF), slag, rice husk ash, and high-reactivity metakaolin (HRM) have been recommended and used for the mitigation of the deleterious effects of ASR in concrete [5–8]. Pozzolanic admixtures are believed to improve the resistance of concrete to ASR by reducing the diffusivity of ions into concrete and through the consumption of $Ca(OH)_2$. However, a complete understanding of how these mineral admixtures influence the chemistry of ASR is still needed.

2. Background

The role of calcium ions in the formation and expansion of gel produced as a result of ASR has been debated by researchers for many years. Some investigators [9,10] support the idea that the presence of calcium ions renders non-expansive gel products and reduces ASR expansion. On the other side, there is an increasing number of investigators [1–4] who support the idea that, even though calcium–alkali–silica gels might not be expansive in nature, calcium ions are vital for deleterious ASR expansion to occur.

Powers and Steinour [9] suggested that gel products that are low in calcium are expansive, while gel products

* Corresponding author.

0958-9465/01/$ - see front matter
PII: S0958-9465(00)00096-2

with a high-calcium content are not. They argued that, when silica is initially attacked by OH^- ions, a calcium–alkali–silica product is formed around the reacting aggregate. Further attack of the intact silica inside the aggregate by calcium and alkali hydroxides from the pore solution would continue by the diffusion of these hydroxides through the non-expansive calcium–alkali–silica layer. If the concentration of alkali with respect to the calcium ions in solution is high, calcium ions will not reach the silica particles in the interior of the aggregate fast enough and expansive gels will form. On the other hand, if calcium ions reach the reacting silica fast enough, non-expansive calcium–alkali–silica gels will develop.

Other researchers have proposed different mechanisms in which calcium ions play a fundamental role in expansion due to ASR. Wang and Gillot [3] showed that expansion of mortar bars increased when 9% $Ca(OH)_2$ was added, even in systems incorporating 20% SF. Based on their experiments using opaline aggregates as well as the results published by other researchers, Wang and Gillot proposed a new mechanism that emphasizes the role of $Ca(OH)_2$ in ASR.

Wang and Gillot proposed that during ASR alkali and calcium ions exchange for protons in silanol groups on the surface of the reactive aggregates forming a calcium–alkali–silica complex. Calcium ions accumulate on the surface of reactive aggregates at early stages of ASR, and as the reaction proceeds, further attack of the interior Si–O bonds by OH^- ions takes place. Simultaneously, Na^+ and K^+ ions are exchanged for Ca^{2+} at the surface of the aggregates, and then penetrate into the open silica structure following the hydroxyl ions. As new silanol groups are formed, sodium and potassium ions are exchanged for protons (H^+) of these silanol groups. An alkali–silica colloidal compound is formed that is capable of absorbing water and developing pressure. Finally, calcium ions penetrate the expanded structure and partially exchange for alkali ions, releasing them into the pore solution for further attack on any remaining reactive silica.

As pointed out by Wang and Gillot, from the above mechanism it should be expected that alkali and calcium ion concentration gradients in the reacting aggregate would develop as ASR occurs. The calcium ion concentration should be highest at the aggregate boundary and decrease towards the center of the aggregate, while alkali concentrations should increase towards the inside reaching a maximum and then decrease.

Recently, other authors showed data that strongly support the idea of the negative influence of calcium ions on ASR. Thomas et al. [1] showed that the addition of $Ca(OH)_2$ increased the expansion of mortar bars even in the presence of fly ash. The studies presented by Thomas et al. showed that gels from deteriorated specimens exhibited a particular calcium band surrounding inner alkali and silica-rich bands. In addition, Thomas and co-workers showed that extensive reaction had occurred in specimens incorporating 40% fly ash. However, these specimens did not expand significantly, and the calcium band present in deteriorated specimens was now absent. The investigators suggested that the absence of calcium in alkali–silica gels rendered products of low viscosity that can intrude into the surrounding paste without developing excessive stresses.

The studies presented in this report explore the influence of HRM and SF on the expansion due to ASR. In addition, the chemistry of ASR gel products was examined using SEM techniques, which include X-ray microanalysis. Our emphasis in this study was to illuminate possible links between calcium content in gel products and expansion.

3. Experimental

3.1. Materials

A high-alkali cement (0.46% Na_2O, 1.06% K_2O, 1.17% Na_2O eq.) was used in all the mixes. The SF used in this investigation was a condensed microsilica from Elkem with a SiO_2 content of 93%. The reported oxide composition ($Al_2O_3 + SiO_2 + Fe_2O_3$) of the HRM was 95.3%.

Dolomitic limestone was used as inert aggregate in all mixes, while Beltane opal was used as reactive aggregate in the alkali-reactive specimens at a substitution ratio of 5% by total weight of aggregate. Five percent is the pessimum content for Beltane opal. All mix proportions and aggregate gradations conformed to the specifications set forth in ASTM C 1260-94 "Standard Test Method for Potential Alkali Reactivity of Aggregates, Mortar Bar Method".

3.2. Sample preparation

Four different mortar mixes were prepared as shown in Table 1. All mixes were prepared with a water-to-cementitious materials ratio of 0.56 and an aggregate-to-cement ratio of 2.25. The Control A mix contained 100% inert aggregates and no mineral admixture. Five percent of the total aggregate content was substituted by Beltane opal in the other three mixes. Ten percent of the total weight of cement was replaced by SF and HRM in the mixes labeled SF and HRM, respectively. The Control B mix contained high-alkali cement and reactive aggregate, but no mineral admixture.

Four mortar bars ($25 \times 25 \times 280$ mm^3) were cast from each mix; two of the bars incorporated end steel

Table 1
Mix proportions for mortar specimens

Mortar mix	Silica fume content (% of cement wt.)	High-reactivity metakaolin (% of cement wt.)	Beltane opal (% of total agg.)
Control A	0	0	0
Control B	0	0	5
SF	10	0	5
HRM	0	10	5

studs and were used for expansion measurements, while the other two bars were used to obtain specimens for SEM/EDS (energy-dispersive spectrometry) examination at different ages. All specimens were cast at room temperature and cured for 24 h at 20°C in a moist room. After demolding, the specimens were stored at 80°C in tap water for 24 h, and then immersed in a 1 N NaOH solution that was kept at 80°C for the remainder of the test.

3.3. Test procedures

The expansion of the bars was measured using a length comparator that conformed to ASTM C 490–93a "Use of Apparatus for The Determination of Length Change of Hardened Cement Paste, Mortar, and Concrete". The initial reading was taken after demolding the specimens (24 h after casting). Then, the zero reading was taken after storing the specimens in tap water at 80°C for an additional 24 h. Immediately after taking the zero reading, the bars were transferred to a 1 N NaOH solution and stored at 80°C. Subsequent measurements were taken at 1, 3, 5, 7, 14, and 21 days after storing the bars in the 1 N NaOH solution.

Two specimens ($25 \times 25 \times 15$ mm^3) per mix were taken from the additional bars at the same time as the expansion measurements were obtained for SEM/EDS examination. A diamond saw was used for this purpose. After cutting, the specimens were immersed in acetone for 1 day. Afterwards, acetone was replaced every other day for a period of 1 week.

Specimens from the Control B, SF, and HRM mixes were analyzed using SEM techniques. Polished sections from specimens taken at 0, 3, and 14 days were prepared for SEM backscattered electron imaging and EDS. Specimens were cut using a low-speed thin diamond saw to produce a relatively flat and smooth surface. Then, the specimens were oven-dried at 60°C for 24 h. After drying, they were impregnated using a low-viscosity epoxy, and then cured at room temperature and 60°C for 12 and 10 h, respectively.

The specimens were coated with gold and analyzed using a Hitachi S-530 scanning electron microscope equipped with a PGT system for EDS analysis. The qualitative analysis included the use of X-ray spectra to study changes in Na, K, Ca, and Si inside reactive aggregates and their surroundings as ASR proceeds. In addition, changes in Na, K, Ca, and Si content in the reactive aggregates and surrounding paste were

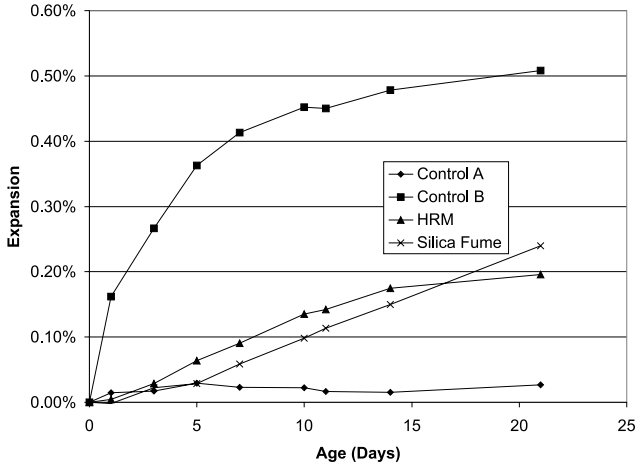

Fig. 1. Influence of HRM and SF on mortar bar expansion over a period of 21 days after immersion in 1 N NaOH at 80°C.

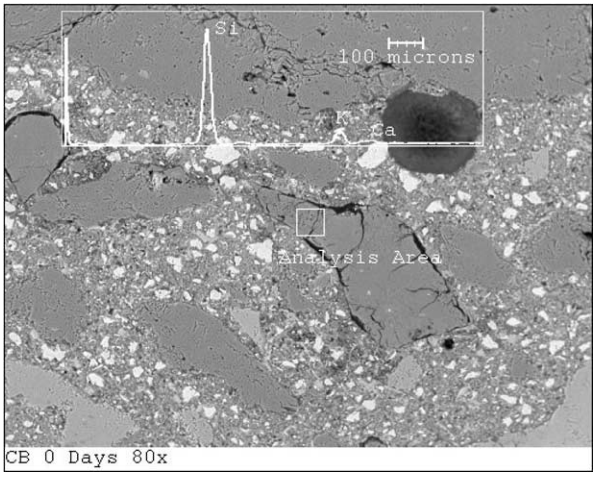

Fig. 2. X-ray spectrum from opal aggregate in Control B sample before immersion in 1 N NaOH.

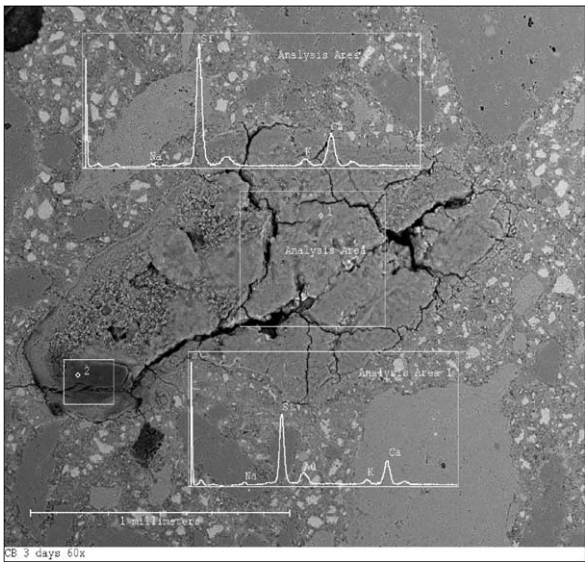

Fig. 3. X-ray spectra from opal aggregate in Control B sample after 3 days of immersion in 1 N NaOH at 80°C.

investigated using quantitative analysis. Furthermore, X-ray maps were obtained to study the distribution of Si, Na, K, and Ca in reacted aggregates and gels.

4. Test results

4.1. Mortar bars expansion

The results of the expansion test (ASTM C 1260) are shown in Fig. 1. As expected, specimens from the Control A mix, which did not incorporate any reactive aggregate, did not show any significant expansion. Control B specimens, which contained reactive aggregate but did not incorporate any mineral admixture, expanded at a fast rate, and reached expansion magnitudes of 0.48% and 0.51% at 14 and 21 days, respectively.

Mortar bars prepared from mixes incorporating HRM or SF showed significantly lower expansion levels at all ages. Specimens incorporating SF expanded 50% less than Control B bars at the end of the test, while a level of expansion 60% lower than that of the Control B specimens was measured in HRM specimens.

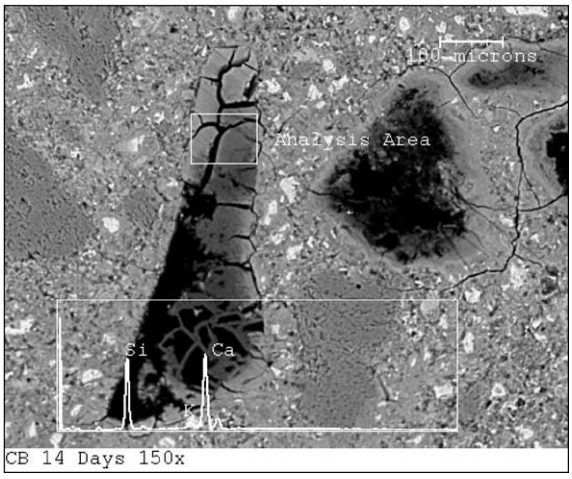

Fig. 4. X-ray spectrum from extensively reacted opal aggregate in Control B sample after 14 days in 1 N NaOH.

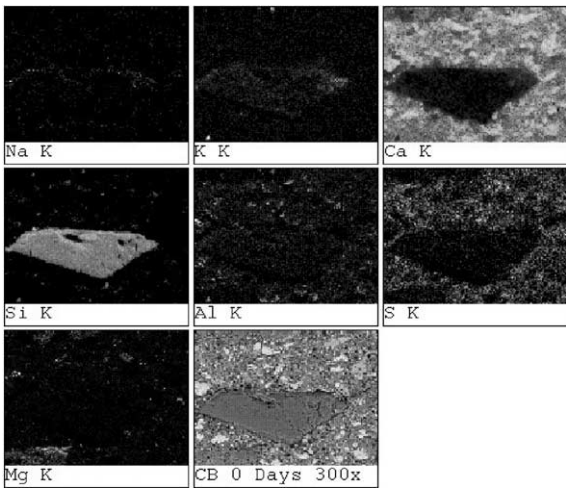

Fig. 5. X-ray dot map of partially reacted opal grain in a Control B sample taken before immersion in 1 N NaOH.

4.2. SEM/EDS analysis

4.2.1. Qualitative analysis

Evidence of extensive reaction and damage was first detected in Control B specimens 3 days after immersion

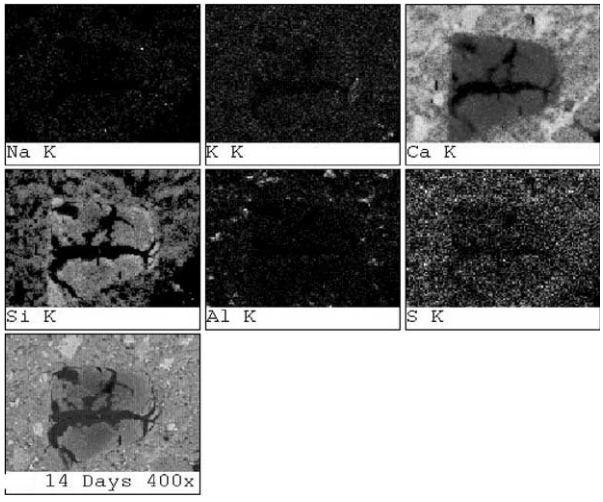

Fig. 6. X-ray dot map from opal aggregate in Control B sample at 14 days after immersion in 1 N NaOH.

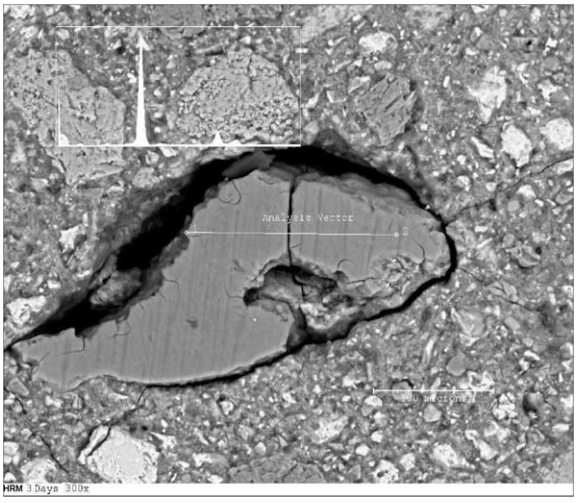

Fig. 7. X-ray spectrum from opal aggregate in HRM sample 3 days after immersion in 1 N NaOH.

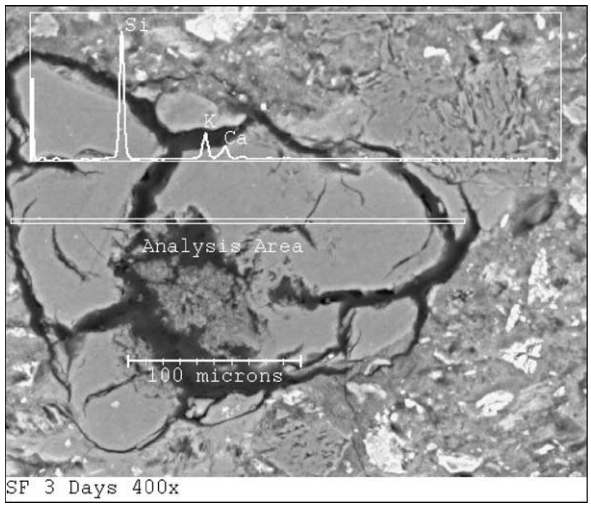

Fig. 9. X-ray spectrum of opal aggregate in sample incorporating SF taken 3 days after immersion in 1 N NaOH.

in 1 N NaOH solution. These observations are consistent with the fact that these specimens had already experienced large expansions at this age (0.26%). Common features in deteriorated specimens included cracks radiating from aggregates, voids filled with gel, and isolated gel deposits in the matrix, refer to Figs. 3 and 4.

X-ray spectra and X-ray maps obtained from opal aggregates in the Control B specimens revealed particular trends in their chemical composition as ASR proceeded (see Figs. 2–4). It was observed that the ratio of calcium peak height to silica peak height increased rapidly over time, while the ratio of potassium peak height to silica peak height decreased to some extent. Sodium peaks were notably low in all the spectra.

Figs. 5 and 6 show the X-ray maps taken from reacted opal aggregates in Control B specimens right before and 14 days after immersion in the alkaline solution, respectively. These pictures illustrate that as the aggregate undergoes ASR, the calcium ions migrate from the surrounding paste into the interior of the affected opal grains. Fig. 5 shows X-ray maps of the partially reacted opal grain from a Control B sample taken before the sample was exposed to 1 N NaOH solution. At this stage the grain is virtually calcium-free and can be easily identified in the center of the calcium

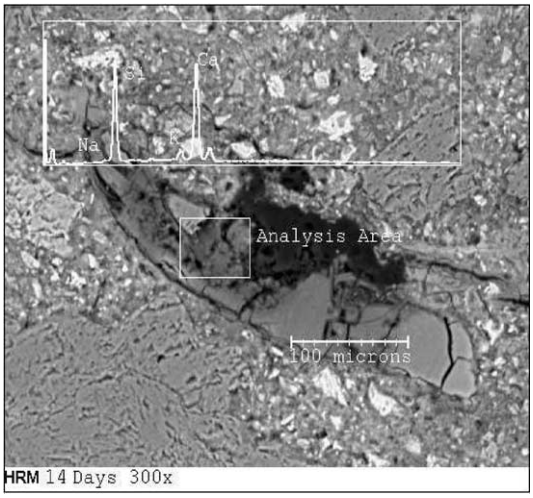

Fig. 8. X-ray spectrum from opal aggregate in HRM sample 14 days after immersion in 1 N NaOH.

Fig. 10. X-ray spectrum of opal aggregate in sample incorporating SF taken 14 days after immersion in 1 N NaOH.

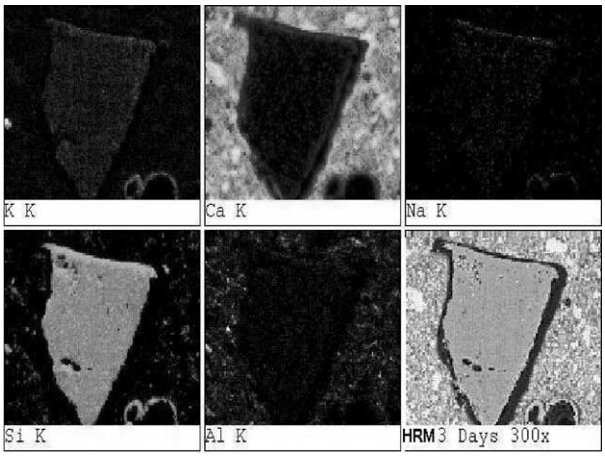

Fig. 11. X-ray dot map from opal aggregate in HRM sample taken at 3 days after immersion in 1 N NaOH.

X-ray map as it looks much darker than the calcium-rich paste that surrounds it. Fig. 6 shows X-ray maps of another opal grain from Control B sample but taken from a specimen that was immersed in 1 N NaOH solution for 14 days. Analysis of the calcium X-ray map of this grain reveals the presence of dark, calcium-free cracks and much lighter-colored (grayish) areas that were penetrated by calcium ions.

When compared to each other, SF and HRM specimens showed similar trends in the chemistry of the reaction products examined. However, marked differences can be observed between these samples and specimens taken from the Control B mix. The calcium to silica peak ratios in X-ray spectra taken from HRM and SF specimens showed the same increasing trend over time as was observed in Control B specimens. Yet, by looking at the X-ray spectra we can see that calcium to silica peak ratios obtained from HRM and SF specimens were considerably smaller than those observed in the Control B mix 3 days after immersion in the alkaline solution (compare Figs. 3, 7 and 8). However, the ratios of calcium to silica peaks observed in HRM and SF specimens after 14 days of exposure were comparable to those observed in Control B specimens, refer to Figs. 9 and 10.

X-ray maps taken from HRM and SF specimens at 3 and 14 days after immersion in the alkaline solution are depicted in Figs. 11–14. Figs. 11 and 12 show X-ray maps of HRM samples taken 3 and 14 days after immersion in the alkaline solution. Analysis of the calcium X-ray map presented in Fig. 11 reveals that after 3 days

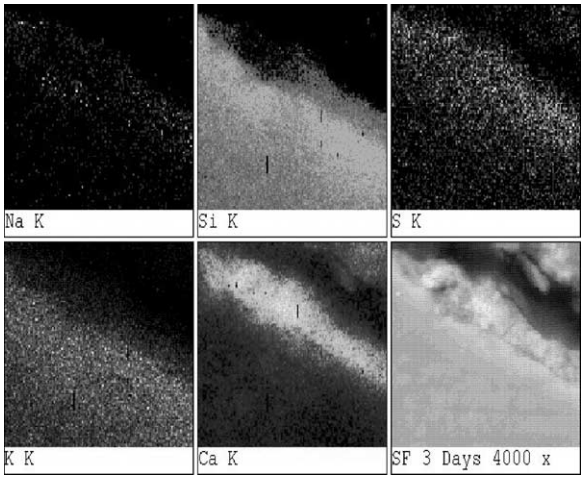

Fig. 13. X-ray dot map of sample incorporating SF taken 3 days after immersion in 1 N NaOH. High-magnification picture (4 K×) of the edge of an opal aggregate.

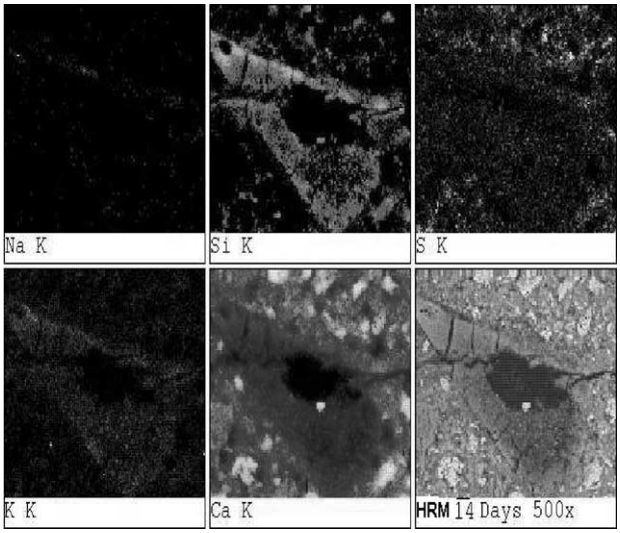

Fig. 12. X-ray dot map from opal aggregate in HRM sample 14 days after immersion in 1 N NaOH.

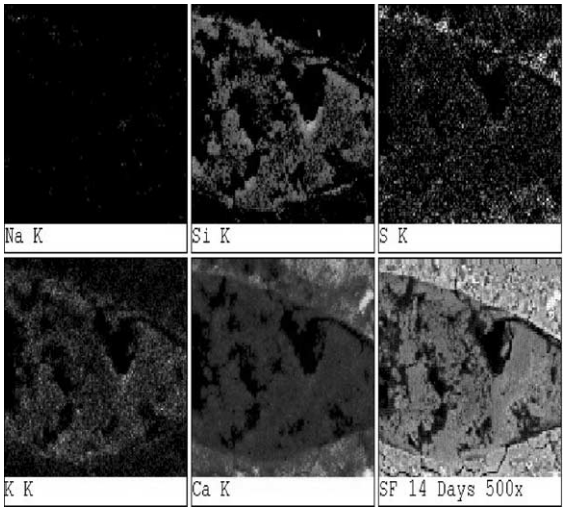

Fig. 14. X-ray dot map from opal aggregate in sample incorporating SF taken 14 days after immersion in 1 N NaOH.

of exposure to 1 N NaOH solution, calcium ions did not penetrate the interior of the reactive aggregate (calcium-free aggregate grain appears as a dark object in the center of the X-ray map). However, the reactive opal particle visible in the calcium X-ray map shown in Fig. 12 (collected from a sample that has been exposed to 1 N NaOH solution for 14 days) is grayish in color, indicating that the entire particle was penetrated by calcium ions.

4.2.2. Quantitative analysis

The elemental composition of reacting aggregates and gel products formed during the reaction was determined using quantitative EDS analysis. Three to five sites showing signs of deterioration were selected randomly in every sample, and X-ray counts were obtained from three to six points located within a selected reacting aggregate or gel.

Fig. 15 shows a plot of calcium content against silica content. These data include information obtained from all the mixes at different ages, and incorporate analyses performed over reactive aggregates as well as gel products. In addition, data from two other different sources [11,12] are also shown on this graph. It can be observed that as the calcium content increases the silica content decreases, irrespective of the system (gel or aggregate) from which the analysis was obtained. A linear regression analysis on the data from the three different sources yielded a high-correlation value ($R^2 = 0.92$) between calcium content and silica content in both reactive aggregates and gels.

As was described in the qualitative analysis section, marked changes in the calcium content of reactive aggregates and gels were detected over time. In order to investigate how HRM and SF influenced these changes, the average calcium to silica ratio of the analyzed spots was plotted versus age for the three different mixes. The control mixes displayed the largest calcium to silica ratio at all ages, followed by SF, and then HRM mixes. Fig. 16 illustrates the changes in calcium to silica ratio with time for the three different systems.

Fig. 17 shows a plot of expansion versus calcium content. This graph includes data obtained from all the systems. The plot shows how expansion follows a linear trend with the increase in calcium content.

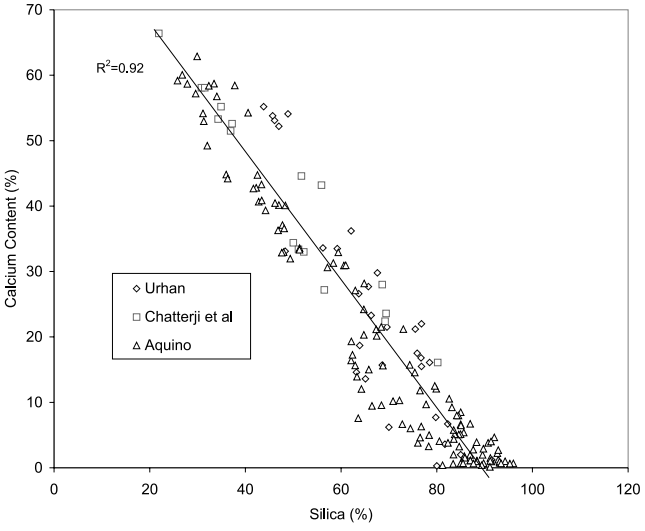

Fig. 15. Calcium versus silica content. Additional data obtained from Urhan [12] (gel sampling only) and Chatterji et al. [11] (gel and reactive aggregate).

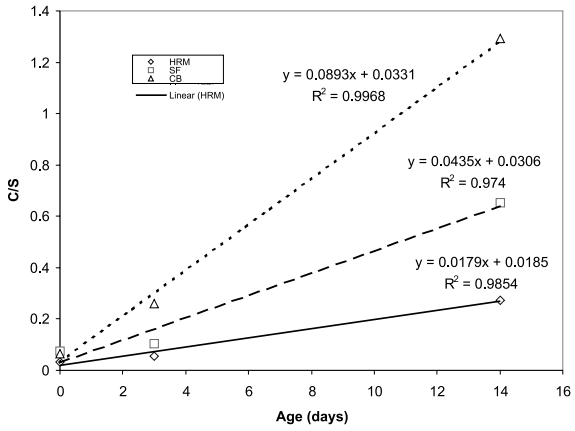

Fig. 16. Calcium to silica ratio against time for the three different mixes.

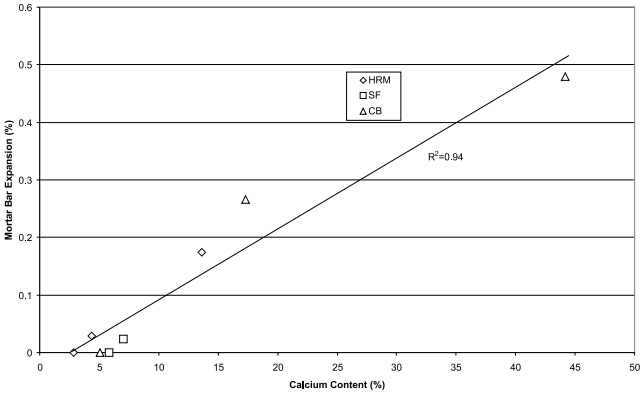

Fig. 17. Expansion versus average calcium content in reactive aggregates.

5. Discussion

In general, SF and HRM performed similarly in reducing expansion due to ASR. Similar results were reported by Walters and Jones [7] in the past. However, it is important to note that specimens containing these

mineral admixtures, despite showing much lower levels of expansion than control specimens at the end of the test (21 days), did in fact continue expanding beyond 21 days. This is most likely due to the fact that the specimens were immersed in a 1 N NaOH solution, which can provide a virtually infinite supply of alkalis. Eventually, any beneficial effect contributed by the admixtures will be overcome and expansion will resume. Therefore, it is important to understand that ASTM C-1260 test has been used for comparison between the performance of the two admixtures and not to draw a conclusion about their absolute effectiveness.

Gillot and Wang [3] have suggested that during the initial stages of the reaction large concentrations of calcium should be observed around the outer boundaries of the reactive aggregates, while potassium and sodium ions should penetrate farther into the amorphous silica structure. As the reaction proceeds, calcium ions penetrate into the aggregate structure, exchanging for sodium and potassium ions. Comparing X-ray maps taken 3 days after exposure, in SF and HRM samples (Figs. 11 and 13), with those taken 14 days after exposure (Figs. 12 and 14) particular trends can be observed in all mixes. Calcium ions were absent in most of the interior of the reactive aggregates at earlier ages and penetrated into reactive aggregates at later ages in all mixes. It can also be observed from the X-ray maps how potassium ions penetrated into the reactive aggregates at earlier ages. These observations clearly confirm earlier results by Gillot and Wang. In addition, Fig. 13 shows a reactive aggregate particle in a specimen containing SF 3 days after immersion in alkaline solution. It can be observed that calcium ions concentrated in a band near the outer edge of the aggregate, while potassium ions concentrated in the inner part of the aggregate.

The linear relationship between calcium and silica contents observed in these experiments may be an indication that alkali–silica gels might be only intermediate products in the process of formation of calcium–alkali–silica gels. More evidence that supports this idea is the fact that this trend holds for both gels and partially reacted aggregates, indicating that low values of calcium to silica ratios imply an early stage of reaction and high values could represent end products of the reaction.

Several authors [1–4] have suggested and shown through indirect tests that calcium ions may be involved in the expansion of ASR gel products. The linear trend shown in Fig. 17 supports the findings of these researchers. Other researchers such as Chatterji [2,11], Gillot and Wang [3], and Thomas et al. [1] have proposed theories that explain how calcium ions participate in ASR and aggravate the expansion.

6. Conclusions

- Silica fume and HRM performed similarly in controlling expansion due to ASR in mortar bars.
- The calcium content of ASR products increased with time in all specimens. However, lower levels of calcium were detected in specimens containing mineral admixtures.
- It was found that as ASR reaction proceeds, the calcium to silica ratio of the reaction products increases following a linear trend.
- The results of the current studies suggest that calcium content in gel products may be linked to expansion.

Acknowledgements

The authors are grateful for the advice and review provided by Prof. S. Diamond at Purdue University and Profs. L. Struble and F. Young at UIUC. Funding for this project was provided by NSF CAREER grant CMS 96-23467 and by the University of Illinois.

References

[1] Thomas MD, Bleszynski A, Roland F. Microstructural studies of alkali–silica reaction in fly-ash concrete immersed in alkaline solutions. ACBM 1998;7(2):66–78.
[2] Chatterji S. The role of $Ca(OH)_2$ in the breakdown of portland cement concrete due to alkali–silica reaction. Cem Concr Res 1979;9:185–8.
[3] Wang H, Gillot JE. Mechanism of alkali–silica reaction and the significance of calcium hydroxide. Cem Concr Res 1991;21:647–51.
[4] Kawamura M, Noriyuki A, Terashima T. Mechanisms of suppresion of ASR expansion by fly ash from the view point of gel composition. In: Cohen M, Mindess S, Skalny J, editors. Materials Science of Concrete – The Sidney Diamond Symposium. Hawaii, 1998. p. 277–84.
[5] Olek J, Aquino W. Role of high-reactivity metakaolin and silica fume in controlling the effects of ASR in concrete. In: Cohen M, Mindess S, Skalny J, editors. Materials Science of Concrete – The Sidney Diamond Symposium. Hawaii, 1998. p. 447–53.
[6] Carrasquillo R, Schumanm D, Farbiaz J. State of the art report on the mechanism of alkali-aggregate reaction in concrete containing fly ash. Research Report 450-2, Center for Transportation Research, Bureau of Engineering Research, Austin, The University of Texas at Austin, 1988.
[7] Walters GV, Jones TR. Effect of metakaolin on alkali–silica reaction (ASR) in concrete manufactured with reactive aggregate. ACI SP 126-50, 1991. p. 941–51.
[8] Gruber KA, Sarkar SL. Exploring the pozzolanic activity of high reactivity metakaolin. World Cem 1996;27(2):78–90.
[9] Powers TC, Steinour, HH. Proceedings of ACI 51, 1955. p. 497.
[10] Wieker W, Hubert C, Heidemann D, Ebert R. Alkali-aggregate reaction – A problem of the insufficient fundamental knowledge of its chemical base. In: Cohen M, Mindess S, Skalny J, editors. Materials Science of Concrete – The Sidney Diamond Symposium. Hawaii, 1998. p. 395–408.

[11] Chatterji S, Thaulow N, Jensen AD, Christensen P. Studies of alkali–silica reaction. Part 3: Mechanisms by which NaCl and $Ca(OH)_2$ affect the reaction. Cem Concr Res 1986;16:246–54.

[12] Urhan S. Alkali–silica and pozzolanic reactions in concrete. Part 1: Interpretation of published results and a hypothesis concerning the mechanism. Cem Concr Res 1987;17:141–52.